



Experimental investigation on stiffened steel plate shear walls with two rectangular openings



Saeid Sabouri-Ghomi, Salaheddin Mamazizi*

Department of Civil Engineering, K.N. Toosi University of Technology, Tehran, Iran

ARTICLE INFO

Article history:

Received 6 March 2014
Received in revised form
20 July 2014
Accepted 8 October 2014

Keywords:

Steel plate shear wall
Opening
Stiffeners
Ultimate shear strength
Energy dissipation

ABSTRACT

One of the most important advantages of steel plate shear wall (SPSW) is to create openings with different sizes and arbitrary locations on the infill plate depending on their application. In this research, the effects of two openings on the structural behavior of SPSWs were studied experimentally. Experimental testing was performed on three one-third scaled single-story SPSW specimens with two rectangular openings under quasi-static cyclic loading. The differences between the three perforated experimental specimens were the interval between two openings and their closeness to the frame columns. The structural parameters of perforated specimens were compared to the similar specimen without any opening. The experimental results were utilized (a) to compare the ultimate shear strength, stiffness and energy absorption of specimens; (b) to evaluate the performance of central, lateral, top and bottom panels; (c) to investigate the effect of distance between the openings and the columns on the formation of plastic hinges on the column flanges; (d) to study the behavior of stiffeners around the openings. Test results showed that the ultimate shear strength, stiffness and energy absorption were the same in all three perforated specimens and the interval between the two openings had no effect on these values. Moreover, existence of openings will lead to reduction in values of structural parameters.

© 2014 Elsevier Ltd. All rights reserved.

1. Introduction

Steel plate shear walls (SPSWs) are an innovative lateral load resisting system capable of effectively bracing a building against both wind and earthquake forces [1]. In addition, one of the advantages of steel shear walls is the providing of openings in the infill plate, which sometimes are required for architectural reasons. The strength and ductility of steel plate shear walls make them very suitable in buildings in seismic high-risk zones [2]. The efficiency of this system was compared with other loading resisting systems such as moment frame and concrete shear wall systems. In general, SPSWs have proven to be effective and economical bracing system for buildings in the range of 15–40 stories [3–5]. During the last three decades, experimental and analytical research on SPSWs systems is mainly focused on the behavior investigation of single- and multi-story thin unstiffened SPSWs with solid infill plates (i.e. without openings). Therefore, limited researches have been conducted on the various types of openings in SPSWs.

Takahashi et al. [6] conducted the first research program on the behavior of stiffened SPSW panels with one stiffened door opening. The test result showed that the stiffness and ultimate shear strength of the steel plate with an opening was supplied well with increase of plate thickness and adequate reinforcement around it. Roberts and Sabouri [7] conducted 16 quasi-static cyclic loading tests on unstiffened slender shear steel panels with centrally placed circular opening. They concluded that the shear strength and stiffness of a perforated panel can be conservatively estimated by applying the linear reduction factor $(1 - D/L)$ to the shear strength and stiffness of a similar solid panel, where D and L are the diameter of circular opening and panel depth, respectively. Vian and Bruneau [8] conducted experimental works on a pattern of multiple regularly spaced circular perforations in the infill steel. Piak [9] presented a formula to predict the ultimate shear strength of perforated steel plates under shear loading. Choi et al. [10] performed an experimental study to investigate the structural capacity of framed steel plate walls with various thin infill plates. Alinia et al. [11] performed a series of numerical analyses to inquire the influence of central and near border cracks on buckling and post-buckling behavior of shear panels. It was implied that discontinuity in tension zones can have significant influence on buckling and post-buckling behavior of SPSWs. Sabouri and Sajjadi [12, 13] tested 4 one story one span SPSWs with a central stiffened

* Correspondence to: Department of Civil Engineering, K.N. Toosi University of Technology, No. 1346, Vali-Asr Street, Tehran 1996715433, Iran.
Tel.: +98 21 88779474; fax: +98 21 88779476.

E-mail address: mamazizi@dena.kntu.ac.ir (S. Mamazizi).

rectangular. They also tested a specimen with one-way stiffener without opening as well as a single frame. It was reported that both the initial stiffness and the ultimate shear strength of the SPSWs reduced with an increase of the width of the opening, compared with identical panels without an opening. Pellegrino et al. [14] studied the influence of the dimension, position and shape of one perforation on the linear buckling and the non-linear behavior of steel plates. Purba [15] proposed a formula to determine the shear strength of a perforated infill plate with the specific perforation pattern proposed by Vian and Bruneau [8].

Valizadeh et al. [16] experimentally obtained that the creation of opening reduced the initial stiffness, strength and energy absorption. Hosseinzadeh [17] investigated the behavior of SPSWs with and without stiffened large rectangular openings. Alavi [18] experimentally developed a formula and verified it for the estimation of shear strength of a perforated and diagonally stiffened SPSW. Bromwich [19] proposed a shear strength model of the infill plate with multiple circular openings based on a strip model for unstiffened SPSW.

In this research, experimental studies were performed on three one-third scaled one-bay single-story stiffened SPSW specimens with two symmetrical rectangular openings under quasi-static cyclic loading. The differences between the three perforated experimental specimens were the interval between two openings and their closeness to the frame columns. Additionally, the experimental results of the specimen without any openings given

in Ref. [12] were used for the comparison of structural parameters. This specimen was similar to perforated specimens in terms of infill plate specifications and frame geometry.

Primary concern was paid to experimental performance of specimens in terms of infill plate buckling, yielding of plates in panels and columns, hysteretic observations. The failure of the different members was investigated according to existence of two same openings with varying locations and different aspect ratios of middle and lateral panels. Moreover the initial stiffness, ultimate shear strength and energy absorption of three experimental specimens was compared together and also with another same specimen without opening [12].

2. Characteristics of the specimens

In this paper three one-third scaled one-bay single-story stiffened SPSWs with two symmetrical stiffened rectangular openings under cyclic loading were examined and experimental results of a same specimen without any openings were used. The perforated specimens were coded as SSW201, SSW202 and SSW203 as shown in Fig. 1. The other SPSW specimen was called DS-SPSW-0% which its infill plate specifications and frame geometry were similar to other specimens except it was without openings as shown in Fig. 2. Stiffeners were installed on the infill steel plate divided it to some sub panels. Sub panel that was

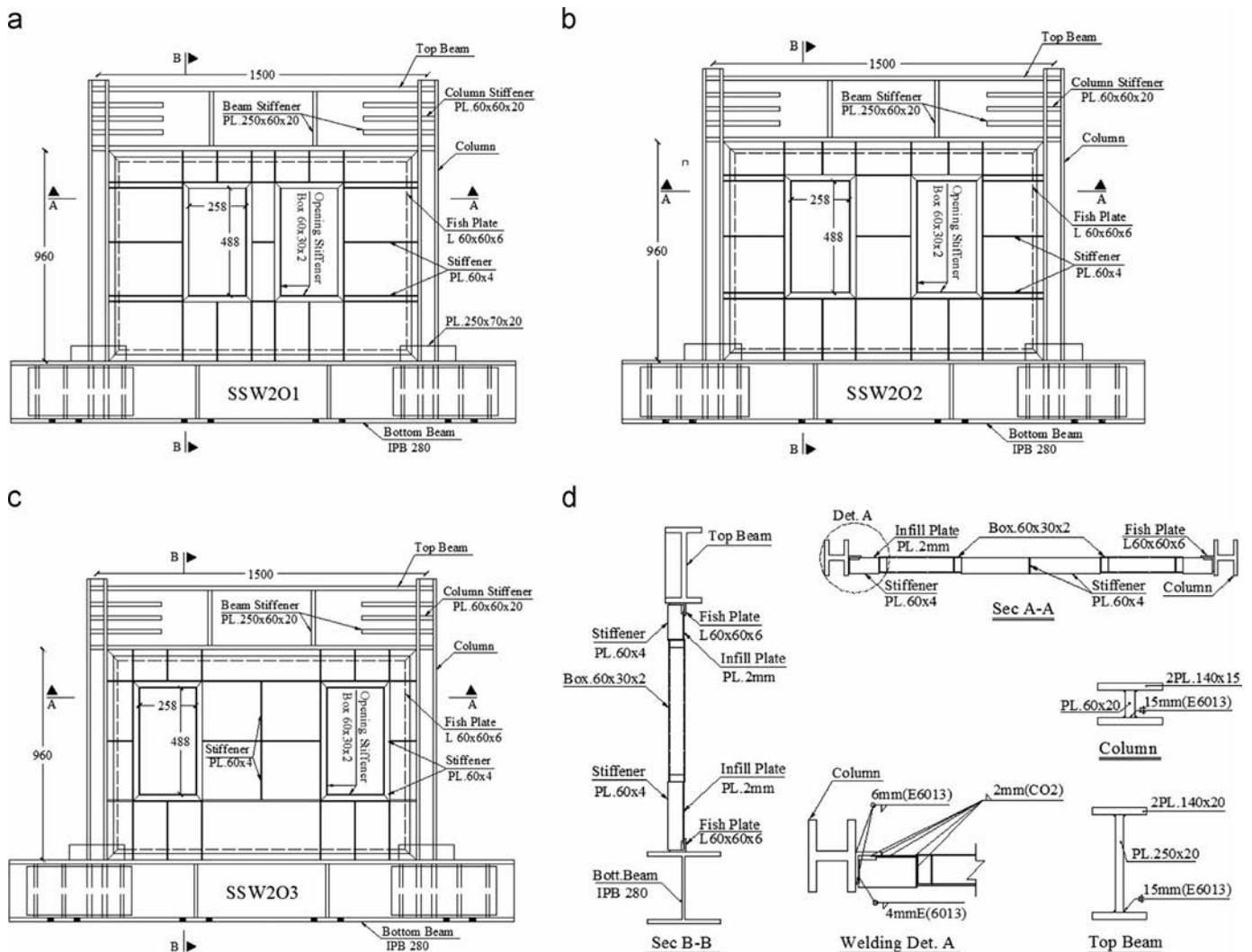


Fig. 1. Specifications and details of perforated specimens. (a) SSW201, (b) SSW202, (c) SSW203 and (d) vertical and horizontal cross sections and welding details.

located between two openings was called middle panel and the sub panels that were located between opening and column were called lateral panels as shown in Fig. 3. This figure also shows the locations of top and bottom panels. The considered variable in these specimens was the interval between openings, which led to different aspect ratios for middle and lateral panels.

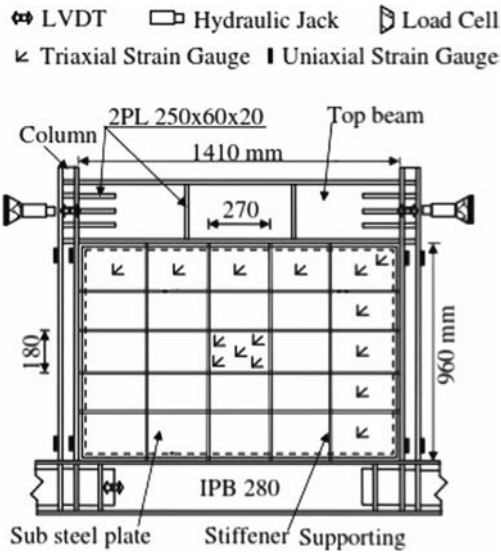


Fig. 2. Specification of DS-SPSW-0% specimen.

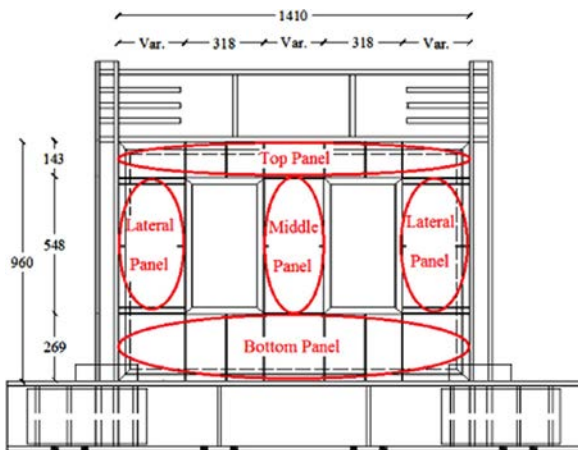


Fig. 3. Typical location of middle, lateral, top and bottom panels and dimensions of panels.

2.1. Specifications and fabrication of specimens and test setup

According to the loading capacity of laboratory actuator, the specimens were designed and fabricated based on PFI (plate-frame interaction) method [20,21]. Fig. 4 shows the fabricated perforated specimens before test. The infill steel plate thickness was taken 2 mm. The distance between the centerlines of columns was 1500 mm and their height was 1250 mm. The inner height and width of the surrounding frame were equal to 960 mm and 1410 mm respectively. The frame was consisted of top beam and two columns, which were built up of plates by welding. The dimensions of the column flange and web were 140 × 15 mm and 60 × 20 mm, respectively and the dimensions of top beam flange and web were 140 × 20 mm and 250 × 20 mm. The internal height and width of the openings was equal to 488 mm and 258 mm, respectively. Fig. 1 shows the specification of specimens, arrangements of different stiffeners, horizontal and vertical cross sections of specimens, dimensions of the columns and top beam, and details of connections and welding. Dimensions of openings and their distance from the bottom and top beams were designed based on architectural considerations. Table 1 shows the width of middle, lateral, top, and bottom panels. The height of panels was similar in all specimens as shown in Fig. 3.

Angle of 60 × 60 × 6 mm was used as fish-plate. For accurate welding between the steel plate and the angle, one side of the angle was milled to 50 mm. The infill plate was lapped over the fish-plate and was welded continuously on the fish-plate. Stiffeners with dimensions of 60 × 4 mm were installed on the one side of the infill steel plate. The philosophy of using the stiffeners on the infill steel plate was to transfer the shear buckling to the sub panels and to increase the shear buckling strength. The required stiffeners on the infill steel plate were optimally designed in terms of layout and the moment of inertia. In addition to the results of eigenvalue buckling finite element method, the following conditions were taken into account for the design of stiffeners:

- (a) The moment inertia of stiffeners and sub panels dimensions were designed such that the local buckling of the sub panels occurred earlier than the global buckling of the steel infill plate [22].
- (b) As shown in Fig. 1, both of the horizontal and vertical stiffeners around openings were connected to the surrounding frame by using stiffeners. Dimensions of sub panels were so that

Table 1
Width of panels (mm).

Specimen	Lateral panel	Middle panel	Bottom panel	Top panel
SSW201	337	100	1410	1410
SSW202	268	238	1410	1410
SSW203	119	536	1410	1410



Fig. 4. Experimental specimens before conducting the test. (a) SSW201, (b) SSW202, and (c) SSW203.

yielding of steel plate occurred before elastic buckling. The interval between openings and columns in SSW201 and SSW202 specimens were somewhat more than SSW203 specimen. Hence, numerical analysis showed that the corresponding horizontal stiffeners should be designed doubly.

The elastic-critical shear buckling stress for local buckling of sub-panels (surrounded by the stiffeners) is obtained from the classical stability equation, by assuming simple support for the plate [23]:

$$\tau_{cr} = \frac{K\pi^2 E}{12(1-\nu^2)} \left(\frac{t}{b}\right)^2 \leq \frac{\sigma_0}{\sqrt{3}} \quad (1)$$

which t , E , ν , d , b and σ_0 is infill plate thickness of, modulus of elasticity, Poisson's ratio, height of sub panel, width of sub panel, uniaxial yield stress, respectively. K is obtained from Eqs. (2) and (3).

$$K = 5.35 + 4\left(\frac{b}{d}\right)^2 \quad \text{for } \left(\frac{d}{b}\right) \geq 1 \quad (2)$$

$$K = 4 + 5.35\left(\frac{b}{d}\right)^2 \quad \text{for } \left(\frac{d}{b}\right) \leq 1 \quad (3)$$

To prevent the large deformation and to provide required stiffness to withstand against the tension field action, a box frame was applied around the openings. Cold-formed steel box of $60 \times 30 \times 2$ mm was used as opening surrounding stiffener that was installed around it which seems more implementable, practically. Hot rolled profile of IPB 280 was used in order to connect the specimens to the laboratory strong floor during the test. The columns bottom of specimens were welded on H-beam top flange. H-beam was connected to the strong floor by 16 high strength bolts. To prevent out of plane displacement and torsional deflection, lateral bracing system including two IPE160 section beams

were designed and installed at the top level on the both sides of the specimen, as shown in Fig. 4.

Complete penetration groove welding was used to create full moment connection between top beam to columns and column base to H-beam. Fillet welding was used for all of other connections. Groove and fillet welds were done by electrode type of E7018 and E6013 respectively. In the welding process of the infill plate was applied CO₂ welding process because the infill plate was of the thin plate (2 mm). The fish-plate was welded to the beams and columns by two-side fillet welding.

2.2. Instrumentations

In order to measure all-important response parameters needed to evaluate the performance of the component or subassembly under study, instrumentation was used to obtain an accurate record of the force and deformation control parameters during the experiment [24].

Applied load, strains, and displacements in key points were monitored by using various instruments. The applied shear force was measured by two load cells that were located on the hydraulic jacks. Linear variable displacement transducers (LVDTs) were placed on the column flange to measure the story drift and column deflections. Furthermore, LVDTs were also used to monitor the out of plane displacement of specimens, the vertical movements of columns and horizontal and vertical displacement of bottom beam. Linear elastic strain gauges were installed on the stiffeners to predict elastic stress. At top and bottom levels of interior and exterior column flanges and surrounding boxes, plastic strain gauges were mounted to determine the strain. Rosette strain gauges were located at different places on the infill steel plate in order to obtain the principal strains and the maximum shear strains. Locations of the rosettes and plastic strain gauge were determined at probable plastic zones in the elements based on the preliminary numerical analysis results. Locations of LVDTs, linear

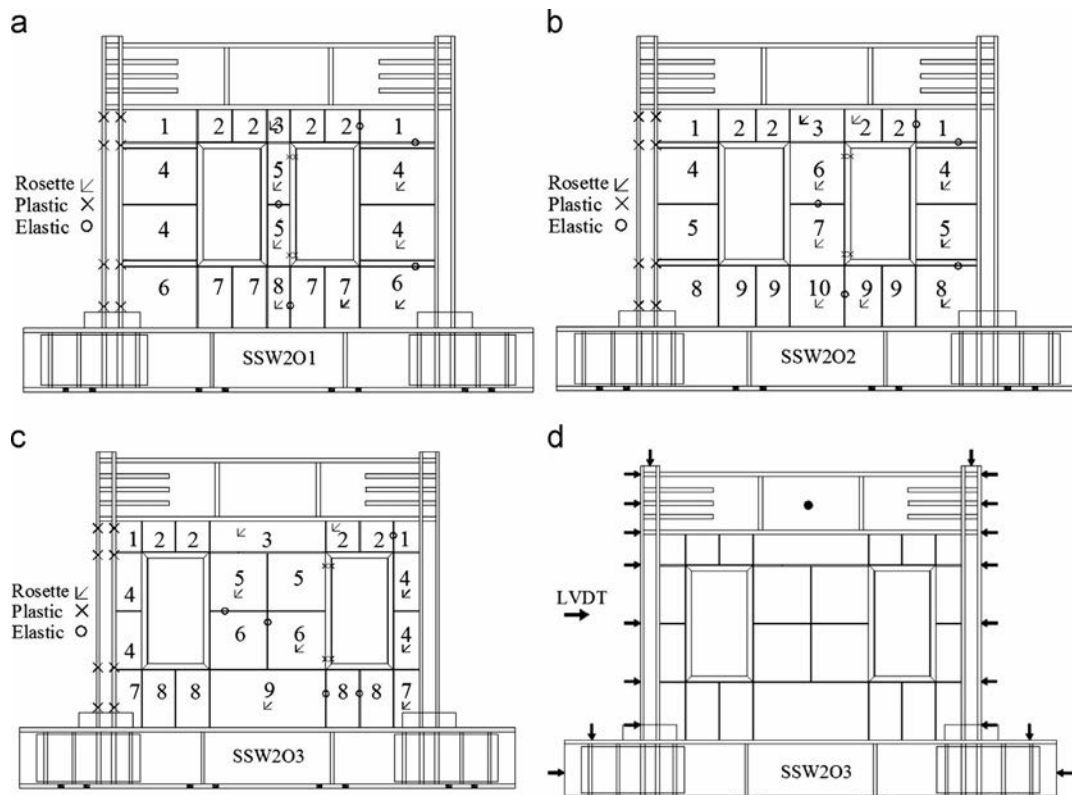


Fig. 5. Code of sub panels and arrangement of instrumentation on perforated specimens. (a) SSW201, (b) SSW202, (c) SSW203, and (d) Arrangement of LVDTs for all specimens.

elastic and plastic strain gauge, and load cells were the same for all three specimens. Nevertheless, the locations of rosette strain gauges in specimens were changed with regard to variation of openings location and panel's dimension. Fig. 5 presents the location of these instruments.

2.3. Material properties

To specify the material properties of the steel plates, the tension test coupon was prepared and tested according to the ASTM A370-05 [25]. Steel material that was used for the infill steel plate was low yield strength, but steel material of the top beam and columns was of high yield strength steel. The type of steel plate was used in the other parts of specimens was ASTM A36 steel. A summary of the coupon tests results are presented in Table 2. The bolts that connected H-beam to the strong floor were of A490 high strength bolt type.

2.4. Cycling loading program

The cyclic quasi-static loading was applied horizontally to the center of the top beam, according to ATC-24 protocol [24]. Before testing, the yielding shear displacement on the infill steel plate was predicted by PFI theoretical method and the numerical method. Later, during the tests, specimens yielded at almost the predicted value, which validated the prediction. Elastic cycles should be performed with force control. According to the protocol, at least three of the elastic cycles should be carried out using force amplitude and in the inelastic region test should be performed under deformation control [24]. No vertical load was applied to the specimens and the test could be stopped when the lateral load dropped below 80% of the maximum load. Fig. 6 shows loading history consists of stepwise increasing deformation cycles, and numbers of cycles were used in each loading step. Five cycles were applied to be performed before the yield point of the specimen.

Table 2
Mechanical properties of steel materials.

Plate thickness (mm)	Yielding stress (MPa)	Ultimate stress (MPa)	Modulus of elasticity (MPa)	Elongation (%)
2	189.5	299.9	206E3	46.2
15	348.2	521.4	208E3	26.9
20	415.7	557.2	209E3	25.2
A36 steel	245.2	384.7	208E3	31.2

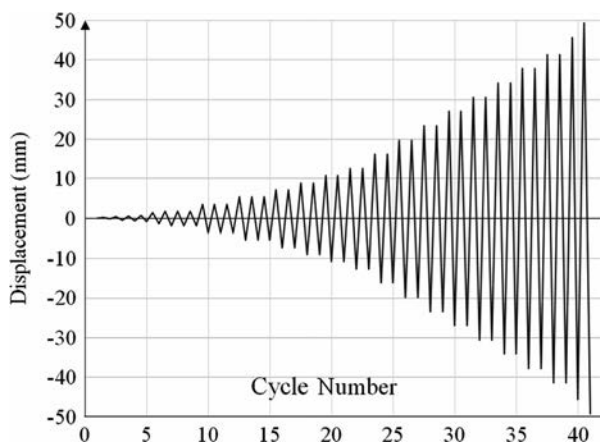


Fig. 6. Lateral loading history according to ATC24.

3. Cyclic behavior of the specimens

The details and descriptions of specimens are described from cycle 6 in the following sections. In the first five cycles loading, installed strain gauges did not show certain yielding on the plate. To present the required description the sub panels of specimens have been numbered as shown in Fig. 5.

3.1. SSW201 specimen

In cycle 6 of loading, the installed rosettes on sub panel 4, showed the initial yielding of the infill plate in 1.3 mm (0.13% drift) horizontal displacement. In this state, the shear force was 201 kN. In cycle 7, the sub panel 6 yielded in 1.7 mm displacement. During cycle 10, sub panels 7 and 5 yielded in 2.5 mm and 2.8 mm displacement respectively, and initial buckling occurred in sub panel 4. At the end of this cycle, crazing was appeared in the box connections. In cycle 13, sub panel 8 yielded in 5.4 mm displacement.

In cycle 14, the exterior column flange yielded at the base in 5.4 mm (0.56% drift) displacement and 430.5 kN shear force. In cycle 16, yielding was commenced in the top of the exterior column flange. In the end of cycle 17, a small separation was appeared in the boxes connection.

During cycle 18, in addition to start of cracking of the boxes connection adjacent to the middle panel, a two-wave buckling was propagated at sub panel 1, as regards the boxes connection at one of its corners had already begun to be cracked as well as angles connection at other corner. This occurrence also took place for sub panel 6 in cycle 20. During cycle 19, crazing was appeared in the angles connection. In 10.8 mm displacement in cycle 20, in addition to buckling of sub panel 6, the exterior column flange yielded at the points corresponding to top and bottom openings edges. In 10.8 mm displacement in cycle 21, buckling occurred in sub panel 7. In this cycle, yielding happened at the top and bottom edges of sub panel 5 in adjacent of the boxes connection (Fig. 7c). In cycle 22, two buckling waves were completely developed and reached to the opposite side in sub panel 1. In cycle 23, in 12.6 mm displacement, tearing occurred in the middle of sub panel 4. During cycle 25, infill plate yielded at sub panel 3.

The ultimate shear strength of 631 kN was obtained in cycle 29th in 23.4 mm (2.4% drift) displacement. In this cycle, the boxes connections was almost separated completely and also steel infill plate begun to rupture at created plastic hinges at top and bottom of middle panel and separation happened in the angle connections.

In cycle 30, buckling and deformation was initiated in the stiffeners attached to boxes connections (Fig. 7b). In cycle 31, cracking was appeared in the connection of column base. In cycle 34, interior column flange yielded at the top and base in 7.9 mm displacement. In cycle 35, rupture of the infill plate was propagated toward the columns from the boxes connections along the prior created buckling waves in sub panels 1 and 6 so that separation of the angles connection contributed it. The rupture of the infill plate at sub panels 1 was more than sub panels 6 because of separation of the angles connection at the top is more than the same connection at the bottom. In cycle 40 at sub panel 1, the infill plate started to separate from attached angle to the top beam. In addition, failure was begun in the fish-plate in the connections of the column base (Fig. 7e). In cycle 41, the infill plate of sub panel 1 was completely ruptured, and in 47.5 mm displacement, the interior column flange yielded at points corresponding to top and bottom edges of the openings.

Eventually, the test was terminated in cycle 41, with failure occurred in the columns base in 50.3 mm (5.2% drift) displacement and strength of 521 kN (Fig. 7d). The view of the specimen after termination of the test was shown in Fig. 7a.

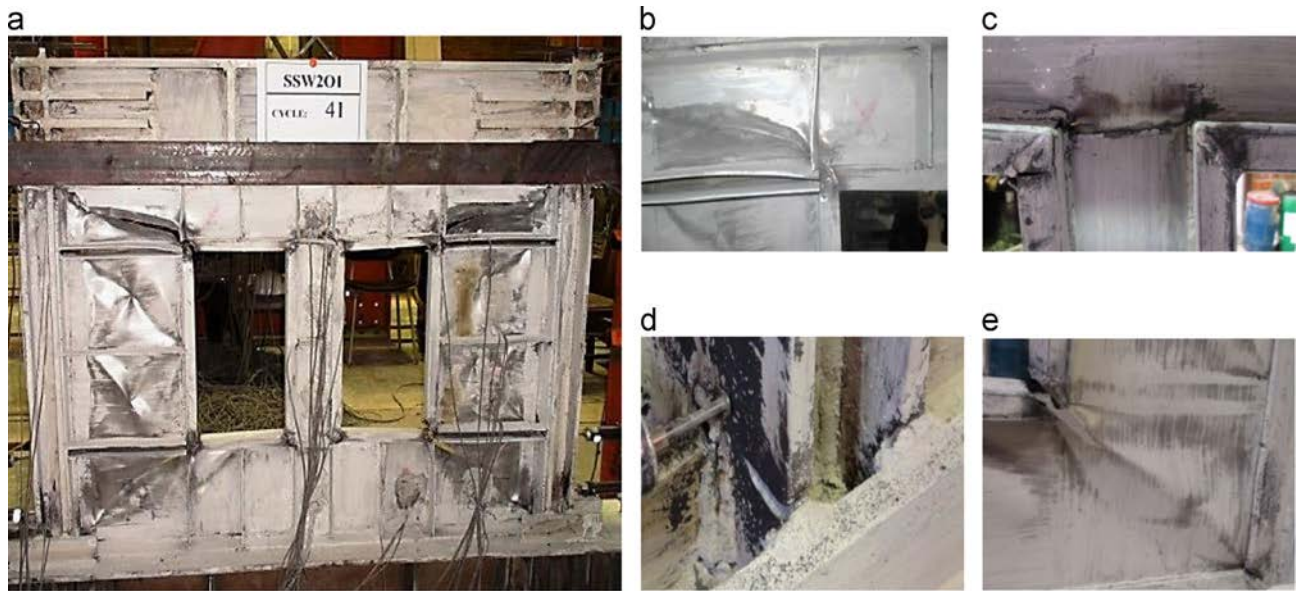


Fig. 7. Details of SSW201 specimen during test. (a) deformation of specimen at cycle 4, (b) plate buckling in subpanel 1, horizontal and vertical stiffeners, (c) plastic hinges at top of middle panel, (d) failure in exterior column flange at base, and (e) tearing infill plate in subpanel 6 and separation in boxes and angles connections.

3.2. SSW202 specimen

In cycle 6 of loading, infill steel plate of sub panels 6 and 7 yielded in 1.3 mm horizontal (0.13% drift) displacement and 185 kN shear force. In this cycle, infill steel plate of sub panels 4 and 5 yielded in 1.5 mm displacement simultaneously. In cycle 7, in 1.4 mm displacement, yielding occurred in sub panel 9, and in the next cycle, sub panel 8 yielded in 1.8 mm displacement. During this cycle, first initial buckling was observed in sub panels 4 and 5 simultaneously. During cycle 11, sub panels 6 and 7 buckled. During cycle 13, sub panels 3 and 10 yielded in 5 and 5.5 mm displacement, respectively. In cycle 14, crazing was appeared in the box connections.

The exterior column flange yielded at the base in 5.7 mm (0.59% drift) displacement in cycle 15. In the end of cycle 16, rupturing was initiated at the connection between the infill plate and boxes in sub panels 1 and 8, and infill plate buckled in these sub panels.

In cycle 22, exterior and interior column flange yielded at the top point in 10.9 mm displacement. Also in 12.8 mm displacement, exterior column flange yielded at the points corresponding to top opening edge. During cycle 23, the buckling wave was initiated in adjacent to the connection between two boxes in sub panel 1 and 8. The buckling wave was fully developed toward the angles connection, and it was caused the boxes connection begin to separate (Fig. 8c).

During cycle 25, failure was commenced in top corner of angles connection. In cycle 26, tearing was observed in middle of sub panel 7 and due to propagation of buckling wave in sub panel 1, rupturing was begun in the sub panel 2 (Fig. 8b). In this cycle, yielding of the infill plate was developed at the top and bottom edges of sub panels 6 and 7 adjacent to the boxes connection (Fig. 8d), and vertical stiffeners attached to the boxes connection buckled in sub panel 1 (Fig. 8b).

The ultimate shear strength of 616 kN was determined in cycle 28, in 23.4 mm (2.4% drift) displacement was. Also in this cycle, boxes connection was fully separated in one of the openings. In cycle 29, in 10.8 mm displacement, exterior column flange yielded at the point corresponding to bottom edge of opening. In cycle 30, interior column flange yielded at the base in 27 mm displacement. In cycle 32, failure occurred in the other top angles connection and

buckling happened in one of the two horizontal stiffeners attached to the bottom box (Fig. 8c). In cycle 34, the bottom angles connection was cracked, and interior column flange yielded at the top and bottom points corresponding to edges of the opening in 31.6 mm displacement. In cycles 35 and 37, failure occurred at the base columns (Fig. 8e).

In cycle 38, separation of the angles connection on the one hand, and separating of the boxes connection on the other hand, was led to rupture of the infill plate in sub panel 1 along the buckling wave. However, in sub panel 6, rupturing of the infill plate was continued from the boxes connection. Finally, the test was terminated in cycle 42 with the shear strength of 545 kN in 61.5 mm (6.3% drift) displacement. Fig. 8a shows the deformed SSW202 specimen after termination of test.

3.3. SSW203 specimen

In cycle 6 of loading, infill plate in sub panels 5 and 6 yielded in 1 mm and 1.2 mm horizontal (0.1% and 0.13% drift) displacement, respectively. In this step, the shear forces were 170.7 kN and 200.4 kN, respectively. During cycle 8, sub panels 2 and 4 yielded in 1.5 and 1.8 mm displacement, respectively. In cycle 10, yielding occurred in sub panel 9, in 2.9 mm displacement. During this cycle, infill plate initially buckled in sub panels 5 and 6. In cycle 13, sub panel 3 yielded in 1.9 mm displacement. In cycle 15, one of angles connections was cracked and one buckling wave was formed in sub panel 1. In cycle 16, in 5.9 mm (0.61% drift) displacement, the exterior column flange yielded at the base. In this cycle, a buckling wave was formed in sub panel 7. In cycle 17, in 7.2 mm displacement, exterior column flange yielded at the top and tearing took place in infill plate adjacent to the boxes connection towards the columns.

During cycle 20, rupturing occurred in the angles connection in sub panel 1, also the boxes connection was cracked. In this cycle, sub panel 8 yielded in 10.8 mm displacement. In cycle 22, exterior column flange yielded at the point corresponding to bottom edge of opening. In next cycle, the infill plate was ruptured adjacent to the boxes connection in sub panel 5. In cycle 24, in 14.2 mm displacement, both of interior and exterior column flanges yielded at the points corresponding to top edge of opening. In cycle 25, the infill plate was locally ruptured in sub panels 5 and 6. In this cycle, top vertical stiffener attached to the boxes connection buckled adjacent to the column (Fig. 9b). In cycle 28, in

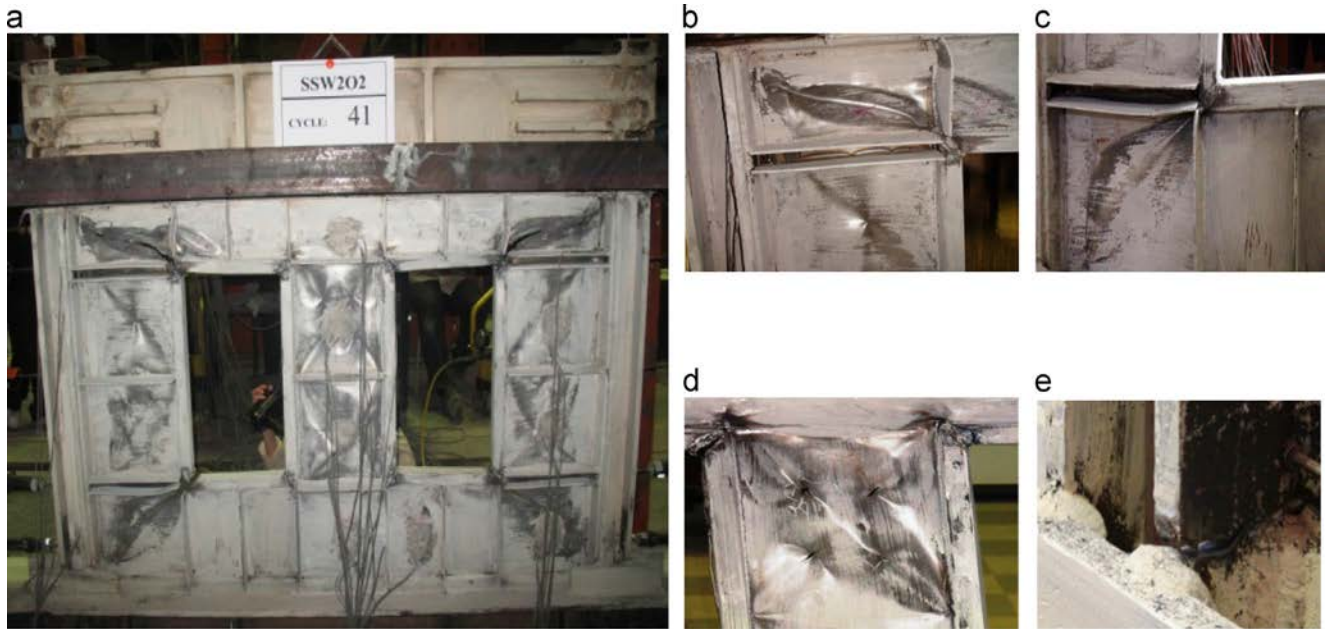


Fig. 8. Details of SSW202 specimen during test. (a) deformation of specimen at cycle 41, (b) plate buckling in subpanels 1,2,4 and vertical stiffeners, (c) plate buckling in subpanels 1,2,3 and vertical stiffener, (d) plate buckling and tearing in subpanel 6, and (e) failure in exterior flange at base column.

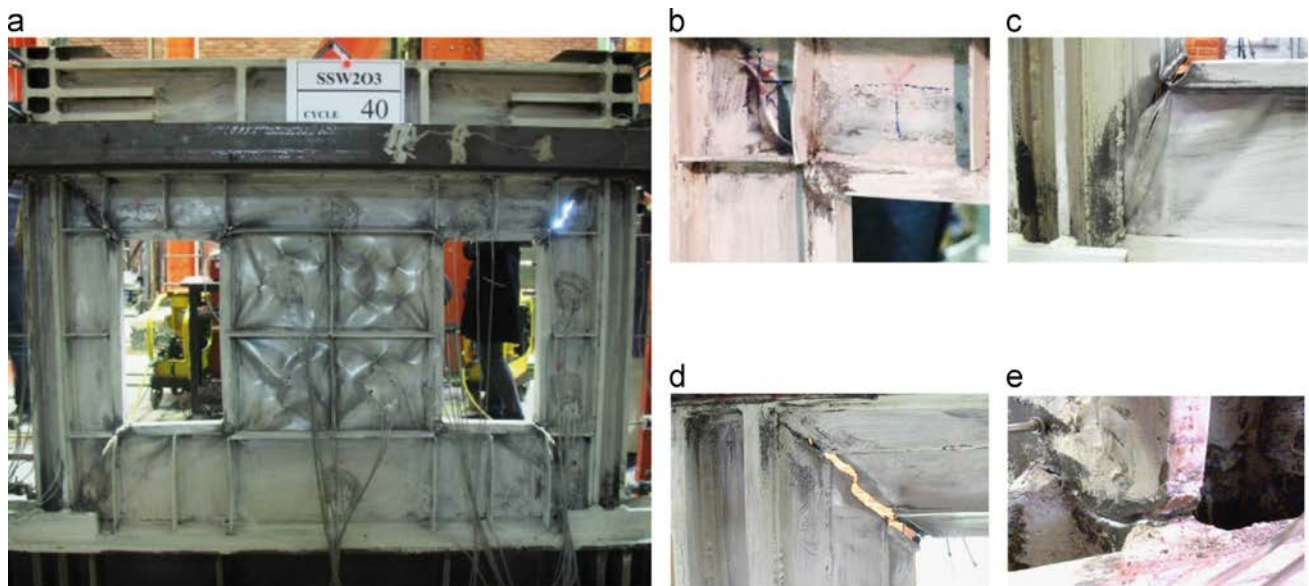


Fig. 9. Details of SSW203 specimen during test. (a) deformation of specimen at cycle 40, (b) plate buckling in subpanels 1 and vertical stiffener, (c) plate tearing in subpanel 7 and separation in boxes connections, (d) plate tearing in subpanel 1 and separation in boxes and angles connections, and (e) failure in exterior flange at base column.

16.8 mm displacement, interior column flange yielded at the point corresponding to top edge of the opening.

The specimen reached to ultimate shear strength of 624 kN in 27 mm (2.8% drift) displacement in cycle 30. In this cycle, boxes connection was completely separated in one of the openings (Fig. 9e). During cycle 33, one of the exterior column flanges failed at the base (Fig. 9c). In cycle 36, in 34 mm displacement, the interior column flange yielded at the base. In cycle 37, the column flange was completely ruptured at the base welding point, as the result the shear strength of specimen was significantly reduced.

In cycle 39, due to increase horizontal displacement, the infill plate in sub panel 1, was completely ruptured along the buckling wave adjacent to the angles connection (Fig. 9d). However, in sub panel 7, the rupture was stopped adjacent to the angle attached to the column (Fig. 9e). Finally, the test was terminated in cycle 40, in

45.8 mm (4.8% drift) displacement with the strength of 573 kN. Fig.9-a shows the deformed SSW203 specimen after termination of test.

3.4. DS-SPSW-0% specimen

In the sixth cycle of the loading, the installed strain gauges on the steel plate showed that the first significant yielding happened at the story shear displacement of 1.58 mm (0.16% drift). The maximum load carrying capacity of the specimen was 808 kN that happened at the story shear displacement of 34.05 mm (3.55% drift). The maximum drift of the specimen was 6.44%. The first sub steel plate local buckling happened at the story shear displacement of 2.7 mm (0.28% drift), then by increasing the story shear displacement, post buckling field developed in all of them. In this



Fig. 10. Deformation of DS-SPSW-0% specimen at 6.44% drift.

specimen, the first steel plate tearing occurred as a very small tear in the middle of the one sub steel plates at 21.6 mm the story shear displacement (2.25% drift) and by increasing the story shear displacement, it was observed in the other sub plates. By increasing the story shear displacement, the tearing in the middle of the sub steel plates increased. No zipping happened between the steel plate and the surrounding frame in the specimen. The tearing gradually developed in the middle of the sub steel plates. In the end of the test, the steel plate shear strength decreased when the sub steel plates almost lost their continuity. The situation of the specimen at the end of the test is shown in Fig. 10.

The strain gauges installed on the columns flanges showed that plastic hinges formed at the top and bottom of the columns between 8.6 mm and 12.9 mm the story shear displacement (0.89% to 1.34% drift).

4. Discussion of results

In the SSW201 specimen, maximum deformation and buckling occurred in lateral sub panels. In other words, lateral panels achieved to the dominant shear mechanism caused by the panel aspect ratio. Hence, lateral panels had a crucial role in energy dissipation. In this specimen, although strain-gauges outputs indicated that the infill steel plate in middle panel yielded during cycle 10th, but it did not have considerable buckling and its contribution to energy dissipation was minimized in the next cycles. With regard to the dimension of the middle panel, in this specimen, the middle panel had bending-dominant.

In SSW202 specimen, middle and lateral panels had almost same dimensions, therefore yielding of the both sub panels occurred at the same displacement approximately as well as local buckling. Moreover, in spite of creation of plastic hinges at the top and bottom edges of the middle panel and their little propagation, this panel actively contributed in energy dissipation.

In SSW203 specimen, the sub panels were located in middle panel had the same buckling behavior after almost simultaneous yielding. Plastic hinges in spite of creation at bottom and top edges of this panel, could not propagate because of the middle panel dimensions. This panel with its shear dominant had a substantial contribution in energy absorption. In this specimen, although the lateral panels yielded during cycle 8, but they did not have a considerable buckling. Especially when sub panel 1 was ruptured, the lateral panels had no contribution in energy absorption anymore, so that these panels performed as a part of the column.

In perforated specimens, top and bottom panels did not have a considerable buckling as well as contribution in energy absorption. Top panel performed more like part of top beam as well as bottom

panel as bottom beam. Eventually rupture was propagated in corners sub panels in top and bottom of specimens.

In perforated specimens because of two following reasons, top and bottom horizontal boxes did not have a noticeable deformation. First, the tension field action was created in sub panels adjacent to horizontal boxes was low; therefore the force produced by post buckling strength was not able to deform the box. Second, vertical stiffener attached to the middle of boxes prevented the deformation of boxes. Nevertheless, deformation of vertical boxes varied depended on the location of the openings. In SSW201 specimen, vertical boxes in vicinity of the middle panel, and in SSW203 specimen, vertical boxes in vicinity of the lateral panel had no noteworthy deformation. In SSW201 specimen, vertical boxes in adjacent of the lateral panel and in SSW203 specimen, vertical boxes in vicinity of the middle panel, and in SSW202 specimen, all of vertical boxes deformed, with regard to large amount of post buckling forces. However, horizontal stiffeners attached to the middle of the vertical boxes had a main role in reducing the horizontal deformation of the box and transform the deformation of boxes into two half-wave at the connection between the stiffener and the box.

One of the main weaknesses of the perforated specimens was the failure of boxes connections that led to the plate rupture and it was propagated towards the angle connection. Rupturing of the boxes connection could be occurred because of following reasons: (a) high stiffness of the box into the infill plate (b) cold formed material of boxes (c) high stress concentration on these points because of welding process.

In all specimens, the infill steel plate tearing happened because of excessive curvature due to the post buckling waves. The excessive curvature of the waves caused reduction in the steel plate thickness on the crest of the waves and the tearing occurred during the cyclic loading. The dimensions of the tears were small and the steel plate kept their continuity. Therefore, they had no significant effect on the shear strength of the specimen. In specimens, no local or global buckling in the columns and no zipping between the steel plate and the surrounding frame happened.

In all specimens, the exterior column flange yielded before of the interior flange in all four measured points. The section modulus of interior column flange was increased by connection of fish-plate.

5. Hysteresis curves and dissipated energy

Hysteresis curves are created by applying cyclic loads to lateral load resisting systems as shown in Fig. 11. Hysteresis loops indicate the strength, stiffness and any kind of local or global instability of specimens. The cyclic tests showed that the specimens had spindle shape and stable hysteretic loops. The application of low yield strength steel in infill plate and high yield strength steel in the frame was caused the infill steel plate to be nonlinear in less shear displacement and improved the hysteresis loops in a sensible manner. In this situation, the columns as main vertical load bearing members, commonly remains safer. From comparison of the shape of loops corresponding to same drift, it was found that the tolerated load was greater in first cycle and was slightly lower in next loops because of residual strains and plastic deformations caused by first cycle.

One of the main properties of the hysteresis curve was its ability to calculation of energy dissipation. The dissipated energy in each loop was evaluated from the area surrounded in the loop. Fig. 12 shows the curves of the dissipated energy for the experimental specimens. The dissipated energy of the perforated specimens is relatively the same as shown in Fig. 12. The dissipated energy of the perforated specimens is similar to unperforated

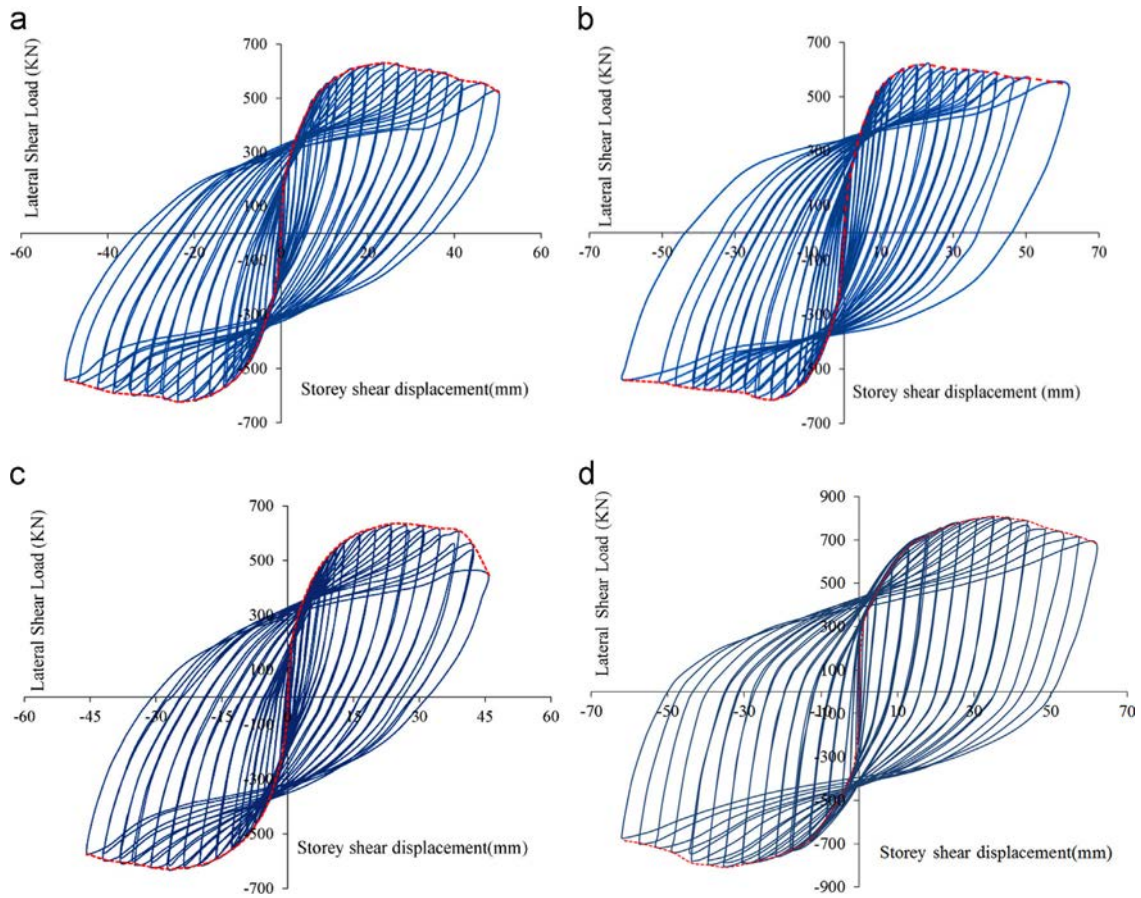


Fig. 11. Hysteresis and envelope curves of specimens. (a) SSW201, (b) SSW202, (c) SSW203, and (d) DS-SPSW-0%.

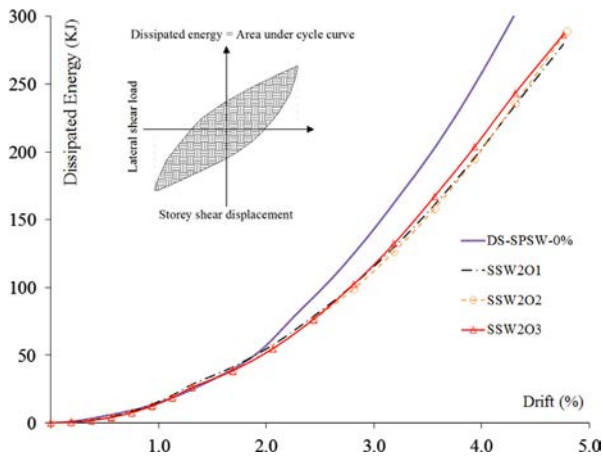


Fig. 12. Cumulative dissipated energy in the specimens.

specimens until 2% drift, whereas the energy absorption of this specimen was increased significantly with increment of drift. The loss of energy absorption in perforated specimens was due to the failure occurred at the corners of the openings that continued along the edge of the columns.

6. Comparison between the results of specimen's structural parameters

For determining structural theoretical parameters like the ultimate shear strength, stiffness and yielding displacements of

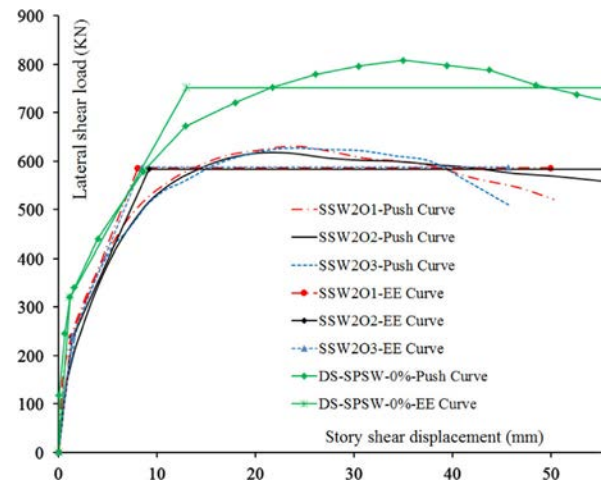


Fig. 13. Tri-linear EE and hysteresis envelope curves of specimens.

the specimens, the Equal Energy curve (EE curve) defined by using of hysteresis envelope curve [12]. The EE curve was obtained by equating the enclosed area under hysteresis envelope curve and EE curve. In the SPSW specimens, the results obtained from the strain gauges showed that, yielding occurred in two stages, the infill steel plate yielding and the plastic hinges forming in the columns. Therefore, EE curve was traced in three lines, which represent these phenomena.

The hysteresis envelope curves of the specimens including the tri-linear EE curves were presented in Fig. 13. The ultimate shear strength and initial shear stiffness of Fig. 13 are given in Table 3. The values of ultimate shear strength and initial shear stiffness

Table 3

Comparison between structural parameters of specimens.

	Ultimate shear strength (kN)	Initial stiffness (kN/mm)
SSW201	585.7	179.1
SSW202	583.8	172.2
SSW203	587.3	170.8
Average of perforated specimens	585.6	174.0
DS-SPSW-0%	751.9	273.5
Difference between average of perforated specimens and unperforated specimen	22%	36%

show a difference 0.6% and 4.6% respectively. It can be observed that EE curves for perforated experimental specimens are very close in initial stiffness and ultimate shear strength. The main important factors for determine of stiffness and ultimate shear strength of the SPSWs were not only related to the following conditions; (a) stiffness of surrounding frame, (b) type of the connection between beam and column, (c) type of the connection between infill steel plate and surrounding frame and, (d) the thickness of main plate, but also it was related to effective width of infill plate. The effective width of infill plate was defined as width of infill steel plate minus width of openings. This width was the same for perforated specimens.

In the DS-SPSW-0% specimen the values of ultimate shear strength and initial shear stiffness are 22% and 36% respectively higher compared to the average of perforated specimens as shown in Table 3. Which means the existence of openings will lead to a considerable decline in the structural parameters, while distance of two openings and distance between openings from columns does not have effect on the structural parameters.

Fig. 13 shows that the shear strength of the surrounding frame, which was caused by the formation of plastic hinges in column, was the same for all of three specimens. It is indicated that distance between the openings and the columns did not have an important influence on location of plastic hinges on the column flanges and, consequently, on the ultimate shear strength of the column.

7. Conclusions

In this research, three one-third scaled experimental specimens were tested under cyclic loads to investigate the effect of existence of two openings on the performance of stiffened SPSWs. The structural parameters of perforated specimens were compared to the same specimen without any opening. Moreover, the following conclusions can be drawn:

- In the perforated specimens, most of the energy dissipation occurred at middle and lateral panels that its magnitude depends on performance type, shear or flexural-dominant. The dissipated energy was much more in the panels with shear-dominant performance. Middle panels in the SSW201 specimen and lateral panels in the SSW203 had flexural-dominant performance. Lateral panels in the SSW201 specimen and middle and lateral panels in the SSW202 specimen had shear dominant performance. In all three specimens, top and bottom panels perform with top and bottom beams and have little effective role in energy absorption.
- Formation of plastic hinges in columns was begun in the exterior flange at the base. Distance between the openings and the columns did not have a significant effect on locations of plastic hinges.
- The connection of horizontal and vertical surrounding boxes was cracked and was ruptured because of higher stiffness of boxes relative to infill plate, cold formed of boxes, and also stress concentration due to much welding process.
- Buckling and deformation in stiffeners attached to the corner of surrounding boxes was much more than stiffeners attached to the middle of boxes.
- Horizontal and vertical stiffeners attached to the middle of the surrounding boxes had an effective role in preventing their deformation.
- Ultimate shear strength, shear stiffness and energy dissipation was equal in all of three perforated experimental specimens with the same effective width of infill steel plate and it was independent of the location of the two openings.
- In the perforated specimens, which the effective width of panels was 63% of unperforated panel, existence of openings will lead to reduce the initial stiffness and ultimate shear strength 22% and 36%, respectively, compared to the unperforated specimen.

References

- Driver RG, Kulak, Elwi AE, GL, Kennedy DJL. Cyclic tests of four-story steel plate shear wall. *ASCE J Struct Eng* 1998;124(2):112–20.
- Elgaaly M. Thin steel plate shear walls behavior and analysis. *Thin Walled Struct* 1998;32:151–80.
- Kulak G. Behavior of steel plate shear walls. In: Proceedings, AISC international engineering symposium on structural steel, Amer. Inst. of Steel Construction, Chicago, 1985.
- Caccese V, Elgaaly M, Chen R. Cyclic testing of 1:4 scale models of thin steel plate shear walls. In: Proceedings of fourth U.S. National conferences on earthquake engineering, California; 1990.
- Elgaaly M, Caccese V, Du C. Steel plate shear walls post-buckling behavior under cyclic loads. In: Proceedings of fourth U.S. national conferences on earthquake engineering, California, 1990.
- Takahashi Y, Takeda T, Takemoto Y, Takagai M. Experimental study on thin steel shear walls and particular steel bracing under alternating horizontal loading. In: Proceedings of the IABSE symposium, resistance and ultimate deformability of structures acted on by well defined repeated loads, Lisbon, Portugal; 1973. p. 185–191.
- Roberts TM, Saburi-Ghomi S. Hysteretic characteristics of unstiffened perforated steel plates shear panels. *Thin Walled Struct* 1992;14:139–51.
- Vian D, Bruneau M. Testing of special LYS steel plate shear walls. In: Proceedings of the 13th world conference on earthquake engineering, Paper No. 978. Vancouver, Canada: Canadian Association for Earthquake Engineering; August 1–6, 2004.
- Paik JK. Ultimate strength of perforated steel plates under shear loading. *Thin Walled Struct* 2007;45:301–6.
- Choi I, Park H. Cyclic test for framed steel plate walls with various infill plate details. In: The 14th world conference on earthquake engineering, China; 2008
- Alinia MM, Hosseinzadeh SAA, Habashi HR. Buckling and post-buckling strength of shear panels degraded by near border cracks. *J Constr Steel Res* 2008;64:1483–94.
- Sabouri-Ghomi S, SRA Sajjadi. Experimental and theoretical studies of steel shear walls with and without stiffeners. *J Constr Steel Res* 2012;75:152–9.
- Sajjadi SRA. Behavior of steel plate shear walls opening. (PhD dissertation). Iran: KNT Univ. of Tehran; 2009.
- Pellegrino C, Maiorana E, Modena C. Linear and non-linear behaviour of steel plates with circular and rectangular holes under shear loading. *Thin Walled Struct* 2009;47:607–16.
- Purba R, Bruneau M. Finite element investigation and design recommendations for perforated steel plate shear walls. *ASCE J Struct Eng* 2009;135(11):1367–76.
- Valizadeh H, Sheidaii M, Showkati H. Experimental investigation on cyclic behavior of perforated steel plate shear walls. *J Constr Steel Res* 2012;70:308–16.
- Hosseinzadeh SAA, Tehranizadeh M. Introduction of stiffened large rectangular openings in steel plate shear walls. *J Constr Steel Res* 2012;77:180–92.

- [18] Alavi E, Nateghi F. Experimental study on diagonally stiffened steel plate shear walls with central perforation. *J Constr Steel Res* 2013;89: 9–20.
- [19] Bhowmick A. Seismic behavior of steel plate shear walls with centrally placed circular perforations. *Thin Walled Struct* 2014;75:30–42.
- [20] Sabouri-Ghomi S. *Lateral load resisting: an introduction to steel plate shear walls*. 1st ed.. Tehran, Iran: Anghizeh Publishing; 2002.
- [21] Sabouri-Ghomi S, Ventura CE, Kharrazi MHK. Shear analysis and design of ductile steel plate walls. *ASCE J Struct Eng* 2005;131(6):878–89.
- [22] Sabouri-Ghomi S, Kharrazi MHK, Mam-Azizi S, Asad Sajadi R. Buckling behavior improvement of steel plate shear wall systems. *J Struct Des Tall Spec Build* 2008;17(4):823–37.
- [23] Timoshenko SP, Goodier JN. *Theory of elasticity*. 3rd ed.. New York: McGraw-Hill; 1970.
- [24] Applied Technology Council. *Guidelines for cyclic seismic testing of components of steel structures*. ATC-24, Redwood City, CA; 1992.
- [25] ASTM A 370-05, SA 370. *Test methods and definitions for mechanical testing of steel products*. *Am Soc Test Mater* 2005:1–47.